Tetrahedron 67 (2011) 4655–4663

Contents lists available at ScienceDirect

Tetrahedron

journal homepage: www.elsevier.com/locate/tet

Azonia spiro polyaza macrocycles containing biphenyl subunits as anion and cation receptors

M. Isabel Burguete [a], M. Paz Clares [b], Enrique García-España [b,*], Santiago V. Luis [a,*], Manel Querol [a], Vicente Martí-Centelles [a]

[a] Department of Inorganic and Organic Chemistry, University Jaume I, Avda. Sos Baynat s/n, E-12071 Castellón, Spain
[b] Instituto de Ciencia Molecular (ICMOL), Departamento de Química Inorgánica, Universidad de Valencia, C/Catedrático José Beltrán 2, E-46980 Paterna, Valencia, Spain

ARTICLE INFO

Article history:
Received 30 November 2010
Received in revised form 7 April 2011
Accepted 15 April 2011
Available online 27 April 2011

Keywords:
Supramolecular chemistry
Macrocycles
Polyaza cyclophanes
Anion recognition
Metal complexes

ABSTRACT

The reaction of *N*-Boc triprotected cyclam with bis(chloromethyl)biphenyl followed by the corresponding deprotection of the nitrogen atoms allows the preparation of receptor **3** containing an azonia spiro subunit. This receptor shows slightly increased basicity than cyclam, in particular for the formation of the appropriate triply charged species as a consequence of the reduced capacity of the structure present in **3** to stabilize the species with lower protonation degrees through the formation of intramolecular hydrogen bonds. The properties of **3** as a receptor for Cu^{2+} and Zn^{2+} and the anions derived from PO_4^{3-} (Pi), $P_2O_7^{4-}$ (PPi), $P_3O_{10}^{5-}$ (TPP) and ATP have been studied by pH-metric titrations carried out in aqueous solution. While Cu^{2+} forms a CuL^{2+} complex and two hydroxylated species of moderate stability, Zn^{2+} forms only hydroxylated complexes. The association constants obtained for the 1:1 A:L anion complexes denote significant stability for Pi, PPi and ATP; the stability of the H_5LA complex found in the case of TPP being lower. ^1H NMR spectra for the ATP:L carried out at pD=5.8 show features attributable to the occurrence of intermolecular π–π stacking between the biphenyl unit of **3** and the adenine ring of the nucleotide. DFT calculations have been carried out to rationalize some of the results found, in particular the remarkable different basicity between receptor **3** and cyclam.

1. Introduction

Polyazamacrocyclic motifs and, in particular polyaza cyclophane moieties, represent a common structural feature for many abiotic anion and cation receptors.[1] The propensity of nitrogen atoms to form coordinative bonds with transition metal cations is at the basis of their behaviour as cation receptors.[2] Recognition of anionic guests by those systems is usually based on the easy protonation, in aqueous media, of the nitrogen atoms to form the corresponding polyammonium compounds containing multiple charges concentrated in a small region as defined by the macrocyclic structure. Moreover, ammonium groups can donate hydrogen bonds to appropriate electronegative atoms of the anionic species.[3,4] However, the occurrence of the different positively charges species is confined to pH limits defined by the protonation constants of the polyamine. Therefore, a second, alternative strategy consists of the development of structures containing quaternized ammonium groups providing a permanent charge independent of the pH of the medium.[5]

The presence of aromatic subunits in polyazamacrocyclic compounds confers interesting characteristics to the resulting ligands. This has been clearly shown, for instance, in the work carried out by our groups in the study of the host–guest chemistry of polyaza[*n*] cyclophanes,[6] cyclic pseudopeptides and related systems.[7] A simple variation on the nature of the aromatic moiety can afford receptors with tailor-made properties, including their capacity to act as fluorescent chemosensors[8] or as simple molecular machines.[9,10] The introduction of biphenyl moieties provides a way to prepare macrocyclic receptors with a dynamic behaviour, in which the dihedral angle of the biphenyl subunit can also contribute to regulate the properties of the resulting receptor. The synthesis and study of biphenyl crown ethers like **1** was reported, some time ago, by Rebek,[11,12] and our group has been involved in the development of different polyaza biphenylophanes like **2**.[13,14] Those biphenylophanes represent a straightforward evolution of the polyaza[*n*] cyclophanes we had previously developed. Nevertheless the preparation of azonia spiro receptors, such as **3** (Chart 1) represents a new approach to the synthesis of biphenyl based receptors. The combination of the quaternized nitrogen atom with the ring

* Corresponding authors. Tel.: +34 964 728 239; fax: +34 964 728 214; e-mail addresses: enrique.garcia-es@uv.es (E. García-España), luiss@qio.uji.es (S.V. Luis).

0040-4020/$ – see front matter © 2011 Elsevier Ltd. All rights reserved.
doi:10.1016/j.tet.2011.04.071

containing the biphenyl fragment can provide those systems with some unique properties. Here we present our results on host **3**, referring to its acid–base properties as well as its capacity to act as receptor for Cu^{2+}, Zn^{2+} and for the anionic species derived from phosphate (Pi), pyrophosphate (PPi), tripolyphosphate (TPP) and 5′-adenosine triphosphate (ATP).

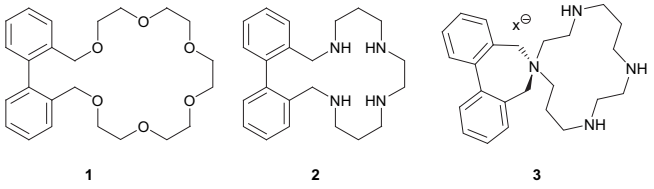

Chart 1. Olyoxa and polyaza macrocycles containing biphenyl subunits.

2. Results and discussion

2.1. Synthesis of receptor 3

The synthesis of receptor **3** was carried out by reaction of bis-(bromomethyl)biphenyl (**4**) with *N*-Boc triprotected cyclam (**5**), which afforded the Boc protected derivative **6**. Using anhydrous K_2CO_3 as the base and equimolar amounts of **4** and **5**, compound **6** was obtained in 86% yield after three days of reaction and following chromatographic purification. Deprotection of the Boc groups was carried out using aqueous HBr in ethanol to give **3** in 80% as the corresponding bromide.

This reaction seems to work also for related systems. Thus, the application of the same synthetic procedure but using the diprotected cyclam **7** and 2 mol of bis(bromomethyl)biphenyl allowed to obtain the diprotected derivative **8** in 52% yield. After deprotection, using the same protocol, the corresponding dicationic polyaza macrocycle **9** was obtained in 90% yield (Scheme 1).

compound **3** (X=Br) were studied by the use of pH-metric titrations. All the titrations were carried out, as has been fully described,[16] at 298.1 K using NaCl 0.15 M to maintain a constant ionic strength. The program PASAT was used for data acquisition.[17] The program HYPERQUAD was employed for the analysis of the electromotive force measurements and for the calculation of the stability constant and the program HYSS was used to obtain the distribution diagrams.[18] The stability constants for the protonation of **3** obtained in this way are presented in Table 1. For comparison, the stability constants for the protonation of cyclam and compound **9** have been also included.[19]

Table 1
Logarithms of the stepwise protonation constants[a] for macrocycles **3**, **9** and cyclam

Reaction[b]	**3**	**9**	Cyclam[d]
H+L=HL	10.27(4)[c]	9.17(4)	11.5
H+HL=H_2L	4.54(4)	3.79(4)	10.5
H+H_2L=H_3L	2.77(4)		1.5
H+H_3L=H_4L			0.9
Log β	17.58	12.96	24.4

[a] Determined in 0.15 mol dm^{-3} NaCl at 298.1 K.
[b] Charges omitted.
[c] Values in parentheses are standard deviations in the last significant figure.
[d] Data taken from Ref. 19.

As can be seen in Table 1, the stepwise protonation constants for **3** follow the expected trends for polyaza macrocycles and polyaza cyclophanes,[20,21] with the presence of one large constant and two smaller ones. This agrees with a situation for which only the first protonation can occur onto a distant enough nitrogen atom from the quaternized nitrogen to minimize the electrostatic repulsion between them. The second and third protonations cannot avoid locating the new charge on a nitrogen atom contiguous to a charged one. When comparing the constants with those reported for cyclam,[19]

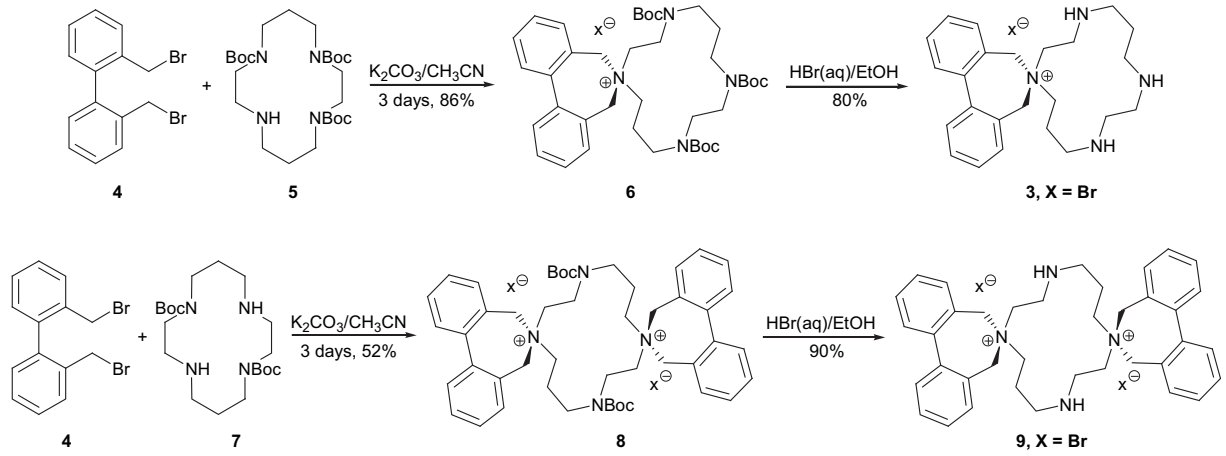

Scheme 1. Synthesis of spiro macrocycles **3** and **9**.

The preparation of *N*-Boc diprotected and triprotected cyclam (**5** and **7**) was carried out following the methodology described by Guilard et al.[15]

2.2. Protonation studies

In order to understand the effect of the quaternized nitrogen atom and the presence of the aromatic rings, a study of the properties of **3** as a receptor for cations and anions in water was undertaken. For this purpose, the protonation behaviour of **3** was initially determined as the first step. Acid–base properties of

It can be observed that the first protonation constant of **3** is comparable with the second protonation constant of cyclam. This is reasonable as the first protonation of **3** corresponds to the formation of a doubly charged species and thus must be compared with the second protonation of cyclam. Nevertheless, the second protonation constant for **3** is significantly larger than the third protonation constant for cyclam ($\Delta\log K$=3.04). The same trend, but to a lesser extent, is observed when comparing the third protonation constant of **3** with the fourth protonation constant of cyclam ($\Delta\log K$=1.87). Interestingly, this phenomenon is still further enhanced in macrocycle **9**. The first protonation of this compound is notably larger than

the third protonation constant of cyclam (Δlog K=7.67) and even larger than the second protonation constant of **3** (Δlog K=4.63). A similar trend is observed for the second constant (Δlog K=2.89).

The former trends are not easy to rationalize. In order to understand the origin of those differences in the values of the protonation constants, we have carried out a computational study at different levels of theory for cyclam and macrocycle **3**, in order to predict the proton affinities of each basic nitrogen atom at the different protonation steps.[22] Initially, a Montecarlo conformational search with the MMFF force field algorithm as implemented in Spartan'04 was carried out for each protonated species. The parameters for this calculation were MAXCONFS=500 WINDOW 50.0 TEMP 20,000 in order to have a wide window of conformers. This conformational search was made for any possible combination of protonated nitrogen atoms for all protonation steps and taking into consideration the presence of symmetry-equivalent protonated structures. The energies obtained for the most stable conformer in each case are presented in Table 2. In the table, the different structures considered have been identified by indicating the protonated nitrogen atoms, which have been numbered consecutively. For **3**, N1 corresponds to the nitrogen atom separated from the quaternary nitrogen by an ethylenic chain.

Table 2
Calculated energies for the minimum energy conformers for each step in the protonation of **3** and cyclam

Cyclam[a]	E_{MMFF} (kcal/mol)	**3**[a]	E_{MMFF} (kcal/mol)
—	37.80	—	87.77
N1	22.82	N1	145.94
N1,N2	94.54	N2	139.07
N1,N3	88.35	N3	140.98
N1,N4	97.86	N1,N2	284.82
N1,N2,N3	249.60	N1,N3	283.33
N1,N2,N3,N4	461.32	N2,N3	286.27
		N1,N2,N3	492.40

[a] Nitrogen atoms being protonated. Nitrogen atoms haven been numbered consecutively. For **3**, N1 corresponds to the nitrogen atom separated from the quaternary nitrogen by an ethylenic chain.

Results in Table 2 allows to predict, for a given protonation step, the proton affinity of each individual nitrogen atom as the difference in energy between the corresponding H_nL and $H_{n-1}L$ species. Thus, this allows predicting for cyclam the expected and known protonation trends. Once the first nitrogen atom is protonated, the most basic is the one located opposite in the cycle (N3), while the third protonation occurs at any of the 2 equiv nitrogen atoms N2 or N4. A similar pattern is determined for receptor **3**. The first protonation takes place preferentially at the nitrogen atom farther away from the quaternized nitrogen atom (N2), which is the most basic. The two remaining unprotonated nitrogens (N1 and N3) are then equally basic for the second protonation. The general process is depicted in Scheme 2.

made with water selected as the solvent.[23] From the energies obtained, the proton affinities could be calculated as described above. According to the presence of clearly defined preferential protonation sites at each protonation step, the proton affinities for the successive protonation steps of cyclam and **3** (Scheme 2) have been gathered in Tables 3 and 4.

Table 3
Calculated proton affinities for each successive protonation step (kcal mol^{-1}) obtained at the different levels of theory for cyclam[a]

Reaction[b,c]	E_{MMFF}	B3LYP/ 6-31 G E_{Gibbs}	B3LYP/ 6-31+G* E_{Gibbs}	B3LYP/ 6-31G $E_{Gibbs\ PCM}$	B3LYP/ 6-31G E_{PCM}[d]
(N1) H+L=HL	−14.98	−255.83	−242.79	−294.81	−306.50
(N3) H+HL=H_2L	65.53	−172.18	−166,16	−293.80	−301.37
(N2) H+H2L=H_3L	161.25	−55.72	−54.09	−253.46	−261.82
(N4) H+H3L=H_4L	211.72	−13.36	−7.52	−269.63	−280.56

[a] All energies were calculated for a minimized geometry at the specified level of theory.
[b] Charges omitted for clarity.
[c] The preferential protonation site considered is indicated in parentheses.
[d] Total energy in solution with all non electrostatic terms as calculated with the SCRF PCM method.

Table 4
Calculated proton affinities for each successive protonation step (kcal mol^{-1}) obtained at the different levels of theory for **3**[a]

Reaction[b,c]	E_{MMFF}	B3LYP/ 6-31G E_{Gibbs}	B3LYP/ 6-31+G* E_{Gibbs}	B3LYP/ 6-31G $E_{Gibbs\ PCM}$	B3LYP/ 6-31G E_{PCM}[d]
(N2) H+L=HL	51.30	−189.45	−182.73	−293.67	−304.46
(N1) H+HL=H_2L	145.75	−87.83	−83.69	−264.44	−274.18
(N3) H+H_2L=H_3L	207.58	−29.23	−23.75	−270.14	−279.67

[a] All energies were calculated for a minimized geometry at the specified level of theory.
[b] Charges omitted for clarity.
[c] The preferential protonation site considered is indicated in parentheses.
[d] Total energy in solution with all non electrostatic terms as calculated with the SCRF PCM method.

The calculated protonic affinities show, for both receptors, the same trends experimentally observed. The only exception should be the last proton affinity calculated at the PCM level for cyclam and **3**, which seem to be overestimated. On the other hand, it is worth mentioning that, in agreement with the experimental results, all levels of theory predict that the second protonation constant of **3** is significantly larger than the third one of cyclam, which corresponds to the formation of a tri-charged species. This is particularly evident in the case of PCM calculations affording essentially the same energy values ($E_{Gibbs\ PCM}$) for the first protonation of **3** and the second protonation of cyclam ($\Delta G \leq 0.3$ kcal mol^{-1}). Those energy values, however, are clearly different when comparing the second protonation of **3** with the third protonation of cyclam. As it is observed experimentally ($\Delta G_{observed}$=4.01 kcal mol^{-1}) monoprotonated **3**, a dicharged species, is predicted to be more basic (ΔG=10.98 kcal mol^{-1}) than diprotonated cyclam.

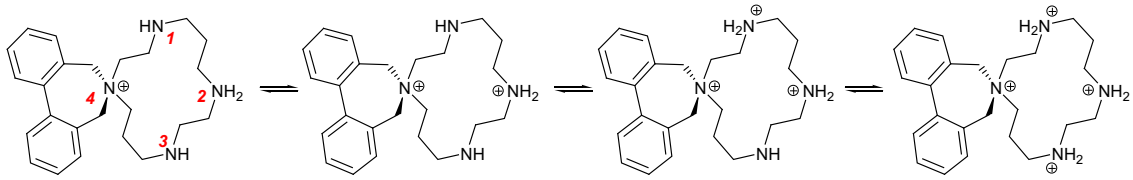

Scheme 2. Preferential protonation sites for the successive protonation steps for compound **3**.

Using the minimum energy conformers as initial structures, for both cyclam and **3**, the geometries were minimized at the B3LYP/6-31G and B3LYP/6-31G* levels of theory in the gas phase using the program Gaussian 03. Additionally, in order to take into consideration the role of the solvent, a minimization at the B3LYP/6-31G level of theory with the polarizable continuum model (PCM) was

The origin of those differences is easily understood when the minimized structures for each protonation step are compared in

detail. The optimized geometries at the B3LYP/6-31G PCM (water as the solvent) obtained from the MMFF minimum energy conformers for the most stable species at each protonation step are shown in Figs. 1 and 2 for cyclam and **3**, respectively.

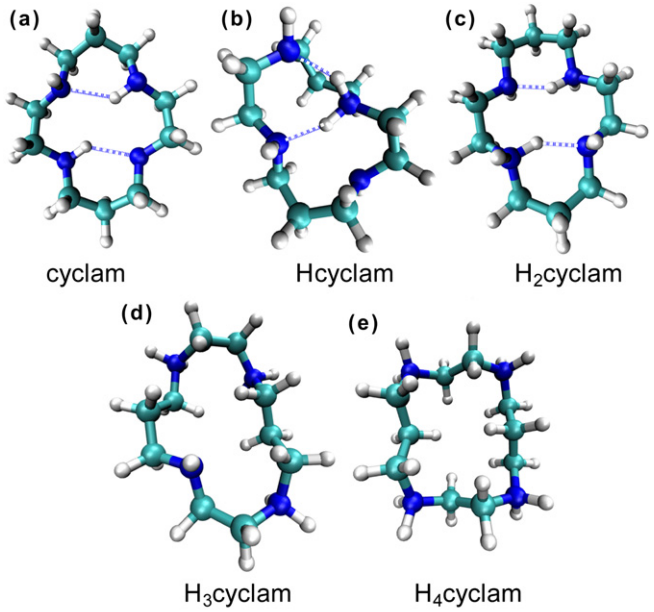

Fig. 1. B3LYP/6-31G PCM (water) optimized geometries from the MMFF minimum energy conformer with the hydrogen bonds showed as dashed lines for cyclam main protonated species. (a) Cyclam. (b) Monoprotonated cyclam. (c) Diprotonated cyclam (at N1 and N3). (d) Triprotonated cyclam. (e) Tetraprotonated cyclam.

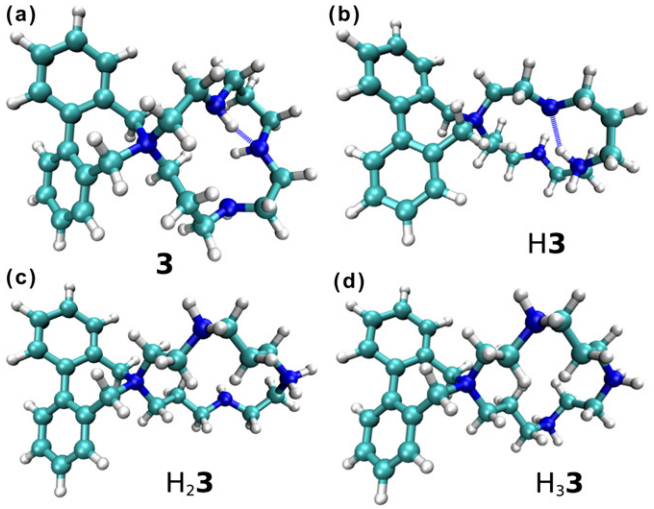

Fig. 2. B3LYP/6-31G PCM (water) optimized geometries from the MMFF minimum energy conformer with the hydrogen bonds showed as dashed lines for **3** main protonated species. (a) Free base. (b) Monoprotonated **3** (at N2). (c) Diprotonated **3** (at N1 and N2). (d) Triprotonated **3**.

It can be observed that, in general, cyclam and derived species are able to form a higher number of intramolecular hydrogen bonds than compound **3** and its protonated derivatives (hydrogen bonds shown as dashed lines in Figs. 1 and 2) in particular for the lower degrees of protonation. Thus, while diprotonated cyclam is predicted to be able to form two hydrogen bonds, the monoprotonated **3** will be forming just one hydrogen bond. In this regard, we must bear in mind that quaternization of a nitrogen atom removes its capacity to form hydrogen bonds. On the other hand, the presence of the azonia spiro junction and the biphenylic subunit seems to reduce the conformational freedom of the polyaza macrocycle, difficulting a proper disposition of nitrogen and hydrogen atoms to favour H-bonding.

The changes occurring in the number of hydrogen bonds at each protonation step are summarized in Table 5. As expected, the number of hydrogen bonds observed in the optimized structures decreases for the structures with a higher degree of protonation, as this is accompanied by a decrease in the number of acceptor atoms available. Nevertheless, the most interesting observation regards the formation of the triply charged species for cyclam and **3** (H_3cyclam and H_2**3**). This protonation step is associated with the stepwise protonation constants of concern: K_3 for cyclam and K_2 for **3**. It can be observed that this step, for cyclam, is accompanied by the unfavourable loss of two hydrogen bonds. In the case of the spiro derivative **3**, only one single hydrogen bond is lost when the second protonation takes place, which is energetically more favourable. This difference seems to be the responsible of the differences measured for the corresponding protonation constants.

Table 5
Hydrogen bonds[a] found in the optimized geometries for reactants and products at the different protonation steps for cyclam and **3**

Reaction	Cyclam		**3**	
	Reactants	Products	Reactants	Products
H+L=HL	2	2	1	1
H+HL=H_2L	2	2	1	0
H+H_2L=H_3L	2	0	0	0
H+H_3L=H_4L	0	0	—	—

[a] Number of hydrogen bonds detected as defined by an N–H distance <2.2 Å; the same results are obtained if the number of hydrogen bonds is defined through the Wiberg Bond Index at the B3LYP/6-31+G* level of theory.[24,25]

2.3. Interaction with cations

Although the macrocyclic cavity present in compound **3** presents a positive charge corresponding to the quaternary ammonium spiranic centre, it still contains three nitrogen donor atoms being able to interact with transition metal cations. Thus, the interaction of **3** with the divalent cations Zn^{2+} and Cu^{2+} was studied by potentiometric titrations in aqueous solution over the 2–11 pH range, by titrating solutions of the metal ions in the presence of the hydrochlorides of the ligands with a strong base. Competition between the metal ions and the protons for binding to the ligand was high enough to permit an accurate determination of the Experimental data. The stability constants obtained are presented in Table 6.

Table 6
Logarithms of the stability constants for the interaction of compound **3** with Cu^{2+} and Zn^{2+} determined at 298.0±0.1 K in NaCl 0.15 mol dm^{-3}

Reaction	Cu(II)	Zn(II)
L+M⇆LM[a]	10.07(1)[b]	
L+M+H_2O⇆LM(OH)+H	2.19(1)	−2.35(3)
L+M+2H_2O⇆LM$(OH)_2$+2H	−8.66(1)	−10.94(3)
LM+H_2O⇆LM(OH)+H	−7.88(2)	
LM(OH)+H_2O⇆LM$(OH)_2$+H	−10.85(2)	−8.59(4)

[a] Charges omitted.
[b] Values in parentheses are standard deviations in the last significant figure.

Formation of an ML complex is only detected for Cu^{2+}, and the value of the constant is about four orders of magnitude smaller than that found for simple tetraaza ligands. The other constants detected correspond to the formation of hydroxylated complexes. In the case of Zn^{2+} only the constants for the formation of the

hydroxylated complexes $[ZnL(OH)]^{2+}$ and $[ZnL(OH)_2]^{+}$ are detected. Thus, for instance, the related biphenylic receptor **2** presents logarithms of the association constants of 18.7 $[CuL]^{2+}$ and 8.7 for $[ZnL]^{2+}$.[13b] The values shown in the Table 6 are more comparable with the ones shown by ligands having only three nitrogen atoms available for the formation of the complex. This is the case of the tetraaza paracyclophane *p*-B323 (see Chart 2) containing the four nitrogen atoms separated by similar aliphatic spacers, in which only three out of the four nitrogen atoms can be simultaneously coordinated to the same metal cation.[26] In this case the values for the formation and hydrolysis constants of $[CuL]^{2+}$ are 13.02 and −9.10 logarithmic units, respectively. Similar values were obtained for related systems, such as the tretraaza metacyclophane *m*-B323.[27] As a matter of fact, the stability constant for the formation of $[CuL]^{3+}$ for **3** (log K=10.07) is still lower than the value of log K=10.89 observed for the interaction of Cu^{2+} with the monoprotonated form of *p*-B323 to give the equally charged species $[CuHL]^{3+}$, reflecting, most likely, the conformational constrains associated to the azonia spiro junction. On the other hand, the constants observed for **3** are about three orders of magnitude higher than values obtained by us recently for some diaza ligands.[7a] The same happens for receptors with three nitrogen atoms located in such a way that only two of them can simultaneously coordinate to the metal, as is the case of the triaza paracyclophane *p*-B33, for which the $[CuL]^{2+}$ complex shows log K=7.97.[28] Overall, it seems that the presence of the quaternary ammonium group produces a clear destabilizing effect on the formation of the corresponding metal complexes, although the data suggest that the three remaining nitrogen donor atoms are able to efficiently coordinate the metal centre.

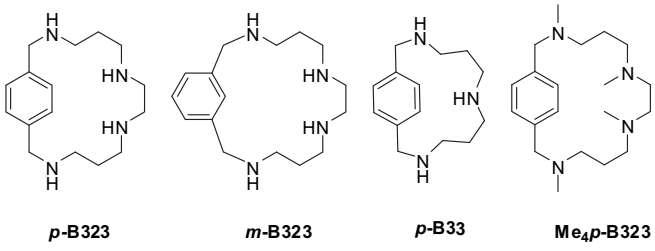

Chart 2. Structures of polyaza cyclophanes *p*-B323, *m*-B323, *p*-B33 Me_4*p*-B323.

The situation is nicely illustrated by the distribution diagrams obtained from the data in Table 6 and shown in Fig. 3. In the case of Cu^{2+}, $[CuL]^{3+}$ predominates over the pH range 4–8, while $[CuL(OH)]^{2+}$ starts to be formed at relatively low pH values (above pH=6) and is predominant at pH values higher than 8. $[CuL(OH)_2]^{+}$ is only formed at pH values higher than 10.

To know how the different basicities of the ligands influence the extent of metal ion complexation, it is useful to build distribution diagrams for the mixed systems Cu:L:L1 and represent the percentages of complexed metal to one or other ligand as a function of pH. As an example, we have done this for the system Cu^{2+}:**3**:*p*-B323 and the plot of complexed Cu^{2+} is shown in Fig. 4.

In such a plot it can be observed that in spite of forming less stable complexes, the lower basicity of **3** with respect to *p*-B323 makes Cu^{2+} to be preferentially complexed to **3** at lower pH values (pH 3–5), while the higher stability of the Cu^{2+} complexes of *p*-B323 makes Cu^{2+} to be bound at a major extent to *p*-B323 above pH 5.

For Zn^{2+}, the complex species are only present at basic pH values, with the dihydroxylated $[ZnL(OH)_2]^{+}$ species being clearly predominant at pH>9. The $[ZnL(OH)]^{2+}$ species is only slightly predominant over the other species in a very narrow pH range in the vicinity of pH=8. The easy deprotonation of the water molecules coordinated to the ML^{3+} complexes as a consequence of the small number of donor atoms provided by the ligand, might be of interest for the development of biomimetic catalytic systems, reproducing, for instance, some of the characteristics of the active site of some enzymes like the HCA.[29]

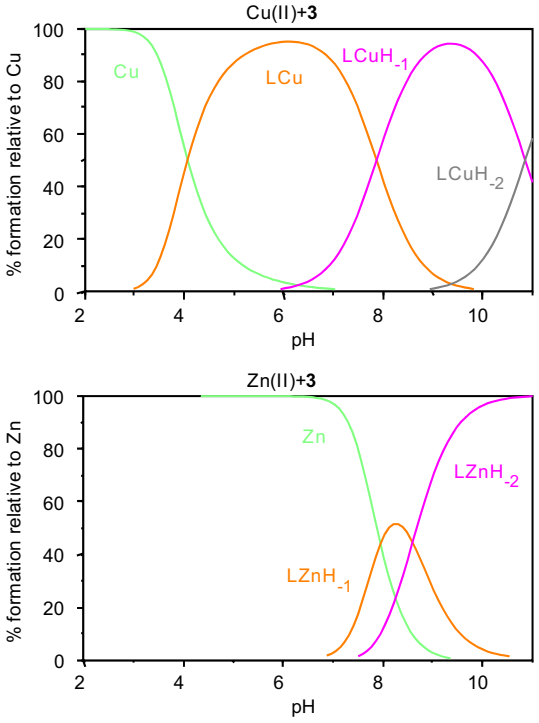

Fig. 3. Distribution diagrams for the interaction of receptor **3** with Cu(II) (top) and Zn(II) (bottom).

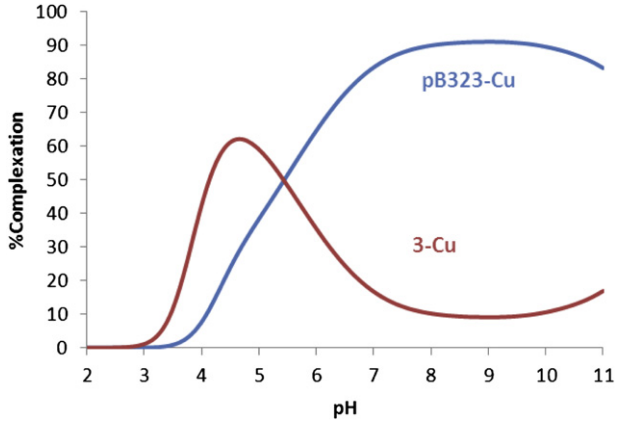

Fig. 4. Plot of the percentages of complexed Cu^{2+} versus pH in the system Cu^{2+}:**3**:*p*-B323 calculated for a 10^{-3} M concentration in the three reactants.

2.4. Interaction with anions

The presence of a quaternary ammonium group can be considered a favourable feature for the interaction with anions at different pH values. In this regard, the interaction of **3** with different phosphate anions (phosphate (Pi), pyrophosphate (PPi), tripolypyrophosphate (TPP) and ATP) was studied by potentiometric titration in aqueous solution over a broad pH range.[30] The association constants for the formation of the respective complexes were

determined at 298.1 K in water and we have chosen 0.15 M NaCl to maintain a constant ionic strength due to the similarity of this concentration with that found in biological tissues. The results obtained are gathered in Table 7 and in the distribution diagrams of Fig. 5.

Table 7
Logarithms of the stability constants for the interaction of compound **3** with the different phosphate anions determined at 298.0±0.1 K in NaCl 0.15 mol dm^{-3}

Reaction[a]	Pi	PPi	TPP	ATP
L+A+H=HLA				12.79(9)
L+A+2H=H_2LA		21.68(3)		20.34(5)
L+A+3H=H_3LA	31.9(1)[b]	28.21(4)		25.54(5)
L+A+4H=H_4LA	36.7(1)	32.97(4)		29.49(5)
L+A+5H=H_5LA	39.92(9)	36.33(3)	34.83(4)	32.66(6)
HL+A=HLA				2.52(9)
HL+HA=H_2LA		3.27(3)		3.69(5)
HL+H_2A=H_3LA	3.4(1)	3.73(3)		5.00(5)
H_2L+H_2A=H_4LA	3.7(1)	3.96(3)		4.43(5)
H_3L+H_2A=H_5LA	4.1(1)	4.54(3)	3.54(4)	4.78(6)

[a] Charges omitted.
[b] Values in parentheses are standard deviations in the last significant figure.

All anions form with **3** adducts of 1:1L:A stoichiometry with protonation degrees varying from 3 to 5 for Pi, 2 to 5 for PPi and 1 to 6 for ATP. However, for TPP just the species H_5L(TTP) was detected in the studied 2.5–11.0 pH range. To analyse the association constants gathered in Table 7, care has to be exerted in comparing the right equilibria and values of stability constants. Since both the receptor and the anions participate in overlapping proton-transfer processes, translating the cumulative stability constants shown in the top entries of Table 7, into representative stepwise ones is not always straightforward. To do so, one has to consider the basicities of **3** and of the different anions involved and assume that the interaction will not be affecting much the pH range of existence of the protonated species of the anions and **3**. If this is considered, the stepwise constants shown in the bottom rows of Table 7 can be inferred. Such constants show that pyrophosphate adducts are more stable than phosphate and tripolyphosphate ones, while they seem to be a little bit less stable than the ATP adducts. However to balance the different basicities and offer proper selectivity criteria, effective constants defined as the quotient at a given pH between the overall amounts of complexed anion and the overall amounts of free receptor and anions are appropriate parameters (Eq. 1).[31]

$$K_{eff} = \sum[H_{i+j}LA] / \sum[H_iL] \times \sum H_jA \quad (1)$$

When these effective constants are calculated, one can observe that according to the conclusions derived from the stepwise constants, PPi and ATP adducts are clearly more stable than the Pi and TPP adducts, however, ATP and PPi present close effective constants with relative stabilities that change with pH (Fig. 6).

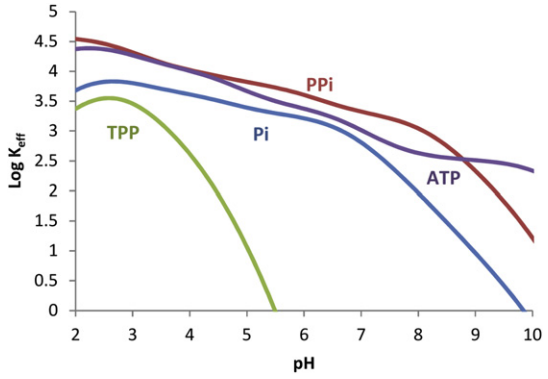

Fig. 6. Plot of the effective constants versus pH for the systems **3**:Pi, **3**:PPi, **3**:TPP and **3**:ATP, calculated for a 10^{-3} M concentration of all reactants.

Another way to visualize these results consists of calculating the distribution diagram for the system Pi:PPi:ATP:**3** for 1:1:1:1 M ratio and represent the percentage of bound anions to **3** as a function of

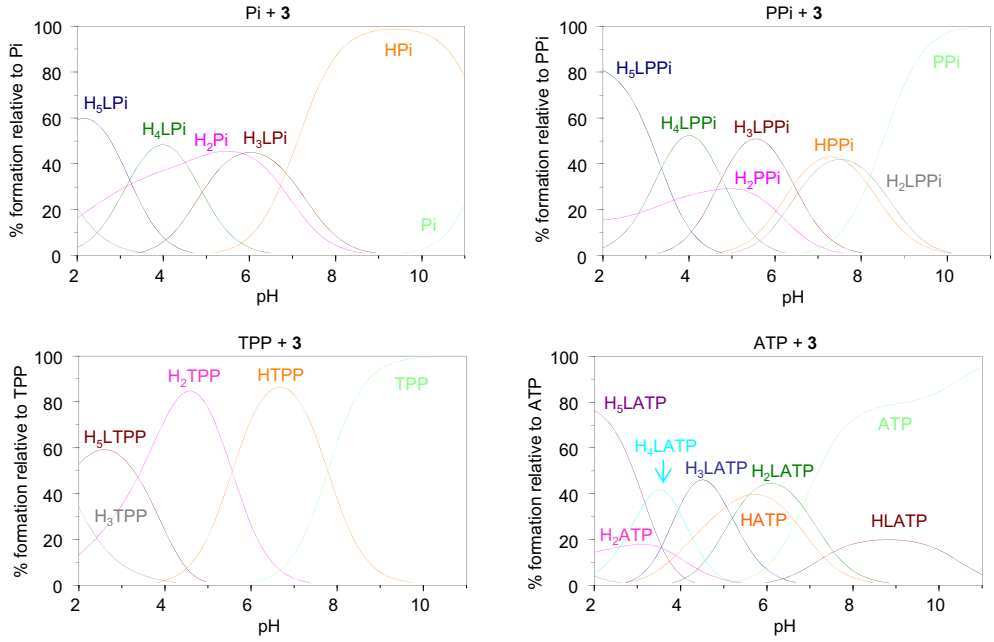

Fig. 5. Distribution diagrams for the interaction of receptor **3** with different anions: Pi, PPi, TPP and ATP^{5-}.

pH (Fig. 7). TPP has not been included due to its much lower interaction. Fig. 7 has a similar profile to Fig. 5, and shows larger extent of complexation of ATP and PPi with respect to Pi over all the pH range covered. Again, it can be seen as the percentages of complexed PPi and ATP depend on pH. The percentages of complexed ATP are slightly larger than those of PPi in the pH range 2.5–6 and above pH 8.5, while the reverse situation occurs from pH 5.0 to 8.5.

It is interesting to analyse the effect of the permanent charge and conformational constraints present in **3** in relation to related non-quaternized cyclophanes. To make such comparisons, the intrinsic charge included in **3** has to be taken into account so that the equilibria considered involve equally charged cationic and anionic species.

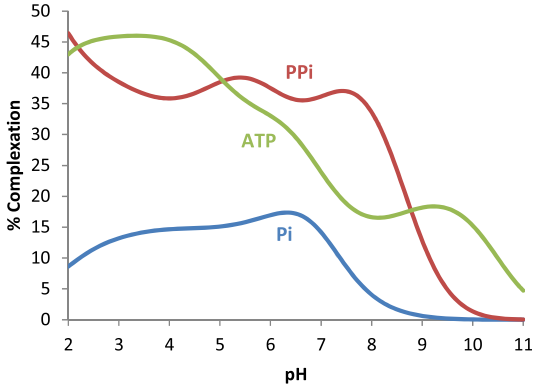

Fig. 7. Plot of the percentages of complexed anion versus pH for a system containing simultaneously **3**, Pi, PPi, and ATP, all of them 10^{-3} M concentration.

Thus, for the tetraaza paracyclophane *p*-B323, a value of 3.87 logarithmic units was obtained for the formation constant of the H_4LPi^{2+} species ($H_3L^{3+}+H_2Pi^-$), which matches quite well with the value of 3.66 logarithmic units obtained for the formation of the H_4LPi^{2+} species calculated for the interaction of H2(**3**)$^{3+}$ with H_2Pi^-.[32] In the case of $P_2O_7^{4-}$ (PPi), the same receptor shows a value of log *K*=4.15 for the formation constant of H_5LPPi^+ ($H_3L^{3+}+H_2PPi^{2-}$) that for **3** can be compared with the value associated to the process $H_2L^{3+}+H_2PPi^{2-}$. The related *N*-tetramethylated cyclophane Me$_4$*p*-B323, that was designed to implement the interaction with anionic species, also displays comparable values: log *K*=3.83 for the equilibrium $H_4L^{4+}+H_2PPi^{2-}=H_6LPPi^{2+}$ and log *K*=4.10 for the equilibrium $H_4L^{4+}+H_2TTP^{3-}=H_6LTTP^+$.[33] Again, the effective constants as defined by Eq. 1 (Fig. 8) provide better ways for establishing selectivity ratios for given pH values. Fig. 7 shows that at acidic pH values the interaction of PPi with 3 is intermediate between those with *p*-B323 and Me4*p*-B323, while at more basic pH values the larger effective constants are those of the tetramethylated receptor.

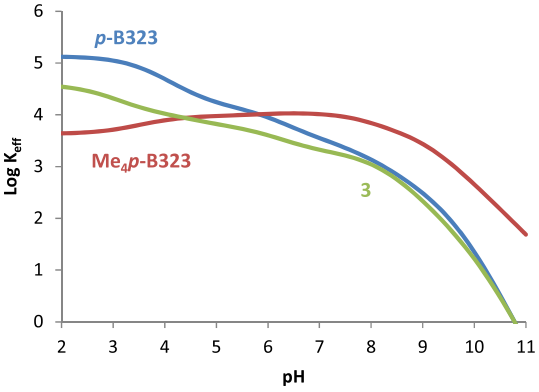

Fig. 8. Plot of the effective constants versus pH for the systems **3**:PPi, *p*-B323:PPi, and Me4*p*B-323:PPi, calculated for a 10^{-3} M concentration of all reactants.

In the case of ATP, **3** displays association constants that are slightly higher than those for *p*-B323 (log *K* 3.82 for $H_4L^{4+}+H_2ATP^{2-}=H_6LATP^{2+}$ in *p*-B323 versus 4.78 for $H_3L^{4+}+H_2ATP^{2-}=H_5LATP^{2+}$ in **3**), while they are smaller than in other receptors better optimized for the interaction with this guest (log *K*=5.4 for $H_4L^{4+}+H_2ATP^{2-}=H_6LATP^{2+}$ in the case of Me$_4$*p*-B323 and 6.01 for **2**). In particular, in the case of the biphenylic macrocycle BF323 (**2**), the related constants are always 1.5–2 orders of magnitude higher.[13b] The plot of the effective constants with pH indicates that in the ATP systems, practically throughout all the pH range covered, the interaction of ATP with **3** is intermediate between that of ATP with *p*-B323 and those observed for the non-quaternized biphenylophane BF323and the tetramethylated Me4*p*-B323 and (see Fig. 9), which interestingly are very similar over all the pH range.

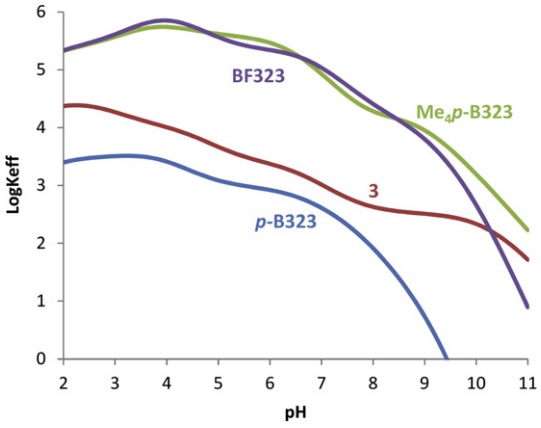

Fig. 9. Plot of the effective constants versus pH for the systems **3**:ATP, *p*-B323:ATP, and Me4*p*-B323:ATP, calculated for a 10^{-3} M concentration of all reactants.

It is worth mentioning that the aromatic subunits seem to play a significant role in the recognition process of ATP by receptor **3**. Addition of a threefold excess of ATP to a solution of **3** in D_2O produces some changes in the aliphatic signals of the receptor that seem to be slightly shifted and clearly broadened. The changes are more significant in the aromatic region, where an appreciable upfield shift of the aromatic signals of **3** is observed ($\Delta\delta$>0.2 ppm) along with some broadening and splitting (Fig. 10). Interestingly, the signals for the aromatic and anomeric protons of ATP also experiment upfield shifts ($\Delta\delta$>0.1 ppm). As expected, the observed shifts are more intense when a threefold excess of the receptor **3** is present in a D_2O solution of ATP ($\Delta\delta$ 0.24–0.31). Minor variations are observed for the aliphatic region of ATP. This evidences that, as

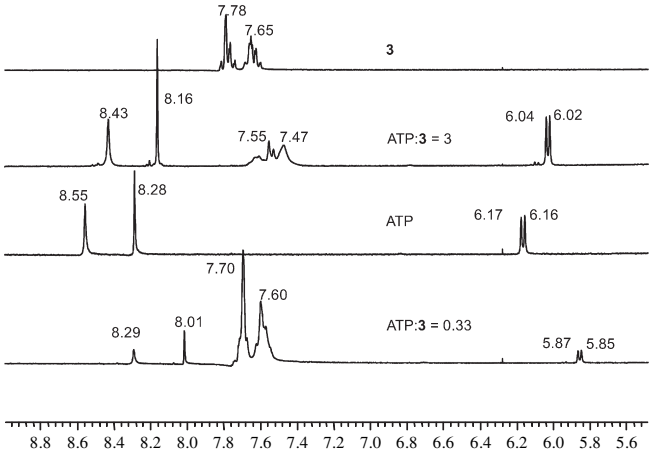

Fig. 10. Aromatic region of the ^{1}H NMR spectra (D_2O) for ATP, receptor **3** and the corresponding complexes in the presence of an excess of ATP (ATP:**3**=3) or an excess of **3** (ATP:**3**=0.33). Chemical shifts are given in parts per million.

in the case of **2**,[13b] and opposite to what is observed for other polyaza[*n*]cyclophanes like Me$_4$*p*-B323,[32] the adduct displays a structure in which the adenosine fragment of the ATP is located above the biphenyl moiety.

3. Conclusions

The incorporation of an azonia spiro junction into the cyclam structure, along with the incorporation of a biphenylic fragment, produces some interesting effects on the properties of the resulting macrocyclic structure (**3**). Although the protonation tendencies of both polynitrogenated systems follows similar patterns, the second and third protonation constants of **3** are significantly higher than the third and fourth constants for cyclam, in which protonated species with the same charge are formed. Detailed computational studies also show the same trends and predict that the higher basicity of some of the protonated species derived from **3** can be associated to the small number of intramolecular hydrogen bonds that are present in those species. The sequential protonation of either cyclam or **3**, passing from H_nL to $H_{n+1}L$, is accompanied by a decrease in the number of intramolecular hydrogen bonds available, which is an unfavourable energetic contribution. This unfavourable factor is, accordingly, less important in **3** than in cyclam as the number of hydrogen bonds lost is lower and could explain its higher basicity. The presence of the quaternized nitrogen atom has an important effect on the interaction of **3** with metal cations. The stability constants with Cu(II) and Zn(II) are lower for **3** than for other related tetraazamacrocycles even when the formation of the monoprotonated species (MHL) is considered for them to take into account the formation of species with the same charge. The conformational constrains associated to the presence of the spiranic junction and the biphenyl fragment can be important in this regard. Nevertheless, the low stability of the metal complexes is accompanied by an easy formation of the corresponding mono- and dihydroxylated species that can be of interest for biomimetic catalytic purposes. On the contrary, the ability of protonated species derived from **3** is much less affected by the presence of the quaternary ammonium group. The association constants determined for the interaction of **3** with different phosphate anions (Pi, PPi, TPP and ATP) reveal that this new compound can act as an efficient anion receptor.

4. Experimental section

4.1. General procedure for the synthesis of *N*-Boc protected aza spiro derivatives

An excess of anhydrous K_2CO_3 was added to a solution of di- or triprotected cyclam (1 mmol) in dry CH_3CN (50 mL) and then a solution of 2,2′-bis(bromomethyl) biphenyl (1 or 2 mmol) in the same solvent was added. The suspension was kept at reflux with strong stirring for 3–4 days. The resulting mixture was filtered and the solvent was vacuum distilled to give a residue that was purified by column chromatography over silica with CH_2Cl_2/MeOH as the eluent.

*4.1.1. 5,7-Dihydro-6H-dibenzo(c,e)azepinium-6-spiro-1′-[4,8,11-tris(tert-butyloxycarbonyl)-1,4,8,11-tetraazatetradecane] bromide (**6**).* Yield (86%). ^{13}C NMR ($CDCl_3$, δ ppm): 27.7, 40.8, 44.0–48.0, 55.1, 55.4, 62.1, 79.1, 79.6, 80.1, 126.3, 128.2, 128.8, 131.0, 132.1, 140.2, 155.0. Calcd for $C_{39}H_{59}BrN_4O_6$: C, 61.65; H, 7.83; N, 7.37. Found: C, 61.65; H, 7.82; N, 7.37. MS-ESI: 680 [M+H].

*4.1.2. 5,7-Dihydro-6H-dibenzo(c,e)azepinium-6-spiro-1′-[4,11-bis-(tert-butyloxycarbonyl)-1,4,8,11-tetraazatetradecane]-8-spiro-6″-(5″,7″-dihydro-6″H-dibenzo(c,e)azepinium) dibromide (**8**).* Yield (52%). ^{13}C NMR ($CDCl_3$, δ ppm): 28.1, 47.5, 47.9, 53.5, 54.0, 55.7, 63.2, 126.3, 129.1, 129.7, 131.9, 132.5, 132.7, 140.3, 141.4, 155.9. Calcd for $C_{48}H_{62}Br_2N_4O_4$: C, 62.74; H, 6.80; N, 6.10. Found: C, 62.77; H, 6.91; N, 6.17. MS-ESI: 380 [M^{2+}].

4.2. General procedure for the deprotection of *N*-Boc protected spiro macrocycles

A concentrated aqueous solution of HBr (9 mL/1 mmol) was added dropwise, at 0 °C, to a solution of the *N*-Boc protected macrocycle dissolved in EtOH (1 mmol/10 mL). Once the addition was completed the stirring was continued at room temperature until no more precipitate was formed. The resulting solid was filtered and vacuum dried.

*4.2.1. 5,7-Dihydro-6H-dibenzo(c,e)azepinium-6-spiro-1′-(1,4,8,11-tetraazatetradecane) bromide (**3**).* Yield (80%). ^{1}H NMR ($CDCl_3$, δ ppm): 2.17 (m, 2H), 2.35 (m, 2H), 3.44 (m, 6H), 3.67 (s, 4H), 3.79–4.04 (m, 4H), 7.50–7.67 (m, 8H). ^{13}C NMR ($CDCl_3$, δ ppm): 19.2, 19.7, 36.9, 37.7, 37.8, 41.0, 41.6, 42.2, 51.3, 55.4, 64.6, 127.0, 129.9, 130.1, 132.8, 133.0, 141.8. Calcd for $C_{24}H_{35}BrN_4$+3HBr+ 1.5$H_2$0: C, 39.53; H, 5.67; N, 7.68. Found: C, 39.55; H, 5.67; N, 7.69. MS-ESI: 380 [M+H].

*4.2.2. 5,7-Dihydro-6H-dibenzo(c,e)azepinium-6-spiro-1′-[1,4,8,11-tetraazatetradecane]-8-spiro-6″-(5″,7″-dihydro-6″H-dibenzo(c,e) azepinium) dibromide (**9**).* Yield (90%). ^{13}C NMR ($CDCl_3$, δ ppm): 21.1, 37.3, 42.1, 51.9, 55.2, 65.2, 127.5, 130.7, 131.0, 133.7, 141.8. Calcd for $C_{38}H_{46}Br_2N_4$+2HBr+2H_2O: C, 49.80; H, 5.72; N, 6.11. Found: C, 50.02; H, 5.81; N, 6.04. MS-ESI: 279 [M^{2+}].

4.3. Computational details

DFT calculations were performed using the Gaussian 03 software package. All structures were computed using density functional theory using the non-local hybrid Becke's three-parameter exchange functional (denoted as B3LYP) with the 6-31G and 6-31G* basis set. Solvation in water was performed with the PCM approximation with the same level of theory. Initially, conformers of the compounds were constructed and computed using the MMFF level of theory with the Montecarlo conformer search implemented in PC Spartan'04.[34] The most stable ones were selected for the full DFT calculation.

4.4. Emf measurements

The potentiometric titrations were carried out at 298.1±0.1 K using 0.15 mol dm^{-3} NaCl as a supporting electrolyte. The experimental procedure (burette, potentiometer, cell, stirrer, microcomputer, etc.) has been fully described elsewhere.[16] The acquisition of the emf data was performed with the computer program PASAT.[17] The reference electrode was an Ag/AgCl electrode in saturated KCl solution. The glass electrode was calibrated as a hydrogen-ion concentration probe by titration of previously standardized amounts of HCl with CO_2-free NaOH solutions and the equivalent point was determined by the Gran method,[35] which gives the standard potential *E*o', and the ionic product of water (p*Kw*=13.73(1)).

The computer program HYPERQUAD was used to calculate the protonation and stability constants.[18] The pH range investigated was 2.0–11.0. The different titration curves for each system (at least two) were treated either as a single set or as separated curves without significant variations in the values of the stability constants. Finally the sets of data were merged together and treated simultaneously to give the final stability constants.

Acknowledgements

Financial support has been provided by MCINN (CTQ2009-14366-C02-01 and CTQ2009-14288-CO4-01) and Fundació Caixa Castelló-Bancaixa (P1-1B-2009-59).

References and notes

1. (a) Beletskaya, I. P.; Averin, A. D.; Bessmertnykh, A. G.; Denat, F.; Guilard, R. *Russ. J. Org. Chem.* **2010**, *46*, 947–967; (b) Steed, J. W.; Atwood, J. L. *Supramolecular Chemistry*, 2nd ed.; John Wiley: Hoboken, NJ, 2009; (c) Gloe, K. *Macrocyclic Chemistry: Current Trends and Future*; Springer: Dordrecht, 2005; (d) Bradshaw, J. S.; Krakowiak, K. E.; Izatt, R. M. *Aza-crown Macrocycles*; John Wiley: New York, NY, 1993.
2. (a) Bazzicalupi, C.; Bencini, A.; Bianchi, A.; Danesi, A.; Faggi, E.; Giorgi, C.; Santarelli, S.; Valtancoli, B. *Coord. Chem. Rev.* **2008**, *252*, 1052–1068; (b) Díaz, P.; García-Basallote, M.; Máñez, M. A.; García-España, E.; Gil, L.; Latorre, J.; Soriano, C.; Verdejo, B.; Luis, S. V. *J. Chem. Soc., Dalton Trans.* **2003**, 1186–1193; (c) Bernardo, M. A.; Pina, F.; Escuder, B.; García-España, E.; Godino-Salido, M. L.; Latorre, J.; Luis, S. V.; Ramirez, J. A.; Soriano, C. *J. Chem. Soc., Dalton Trans.* **1999**, 915–921; (d) Bernardo, M. A.; Pina, F.; García-España, E.; Latorre, J.; Luis, S. V.; Llinares, J. M.; Ramirez, J. A.; Soriano, C. *Inorg. Chem.* **1998**, *37*, 3935–3942; (e) Andres, A.; Bazzicaluppi, C.; Bianchi, A.; García-España, E.; Luis, S. V.; Miravet, J. F.; Ramirez, J. A. *J. Chem. Soc., Dalton Trans.* **1994**, 2995–3004; (f) Bencini, A.; Bianchi, A.; Paoletti, P.; Paoli, P. *Coord. Chem. Rev.* **1992**, *120*, 51–85; (g) Bianchi, A.; Micheloni, M.; Paoletti, P. *Coord. Chem. Rev.* **1991**, *110*, 17–113.
3. (a) Mateus, P.; Bernier, N.; Delgado, R. *Coord. Chem. Rev.* **2010**, *254*, 1726–1747; (b) García-España, E.; Díaz, P.; Llinares, J. M.; Bianchi, A. *Coord. Chem. Rev.* **2006**, *250*, 2952–2986; (c) Sivakova, S.; Rowan, S. J. *Chem. Soc. Rev.* **2005**, *34*, 9–21; (d) Sessler, J. L.; Jayawickramarajah, J. *Chem. Commun.* **2005**, 1939–1949; (e) Auki, S.; Kimura, E. *Chem. Rev.* **2004**, *104*, 769–787; (f) Llinares, J. M.; Powell, D.; Bowman-James, K. *Coord. Chem. Rev.* **2003**, *240*, 57–75; (g) Beer, P. D.; Gale, P. A. *Angew. Chem., Int. Ed.* **2001**, *40*, 486–516; (h) *Supramolecular Chemistry of Anions*; Bianchi, A., García-España, E., Bowman-James, K., Eds.; Wiley-VCH: New York, NY, 1997.
4. See also the recent Supramolecular chemistry of anionic species themed issue: *Chem. Soc. Rev.*; Gale, P., Gunnlaugsson, T., Eds.; 2010; Vol 39, pp 3581–4008.
5. (a) Schmidtchen, F. P.; Berger, M. *Chem. Rev.* **1997**, *97*, 1609–1646; (b) Schmidtchen, F. P. *Angew. Chem., Int. Ed. Engl.* **1981**, *20*, 466–468; (c) Schmidtchen, F. P. *Angew. Chem., Int. Ed. Engl.* **1977**, *16*, 720–721.
6. (a) Hodacova, J.; Aguilar, J.; García-España, E.; Luis, S. V.; Miravet, J. F. *J. Org. Chem.* **2005**, *70*, 2042–2047; (b) Yuan, Y.; Gao, G.; Jiang, Z. L.; You, J. S.; Zhou, Z. Y.; Yuan, D. Q.; Xie, R. G. *Tetrahedron* **2002**, *58*, 8993–8999; (c) Gibson, S. E.; Jones, J. O.; Kalindjian, S. B.; Knight, J. D.; Steed, J. W.; Tozer, M. J. *Chem. Commun.* **2002**, 1938–1939; (d) Heuft, M. A.; Fallis, A. G. *Angew. Chem., Int. Ed.* **2002**, *41*, 4520–4523; (e) Inoue, M. B.; Inoue, M.; Sugich-Miranda, R.; Machi, L.; Velazquez, E. F.; Fernando, Q. *Inorg. Chim. Acta* **2001**, *317*, 181–189; (f) Andrés, A.; Burguete, M. I.; Escuder, B.; Frías, J. C.; García-España, E.; Luis, S. V.; Miravet, J. F. *J. Org. Chem.* **1998**, *63*, 1810–1818.
7. (a) Blasco, S.; Burguete, M. I.; Clares, M. P.; García-España, E.; Escorihuela, J.; Luis, S. V. *Inorg. Chem.* **2010**, *49*, 7841–7852; (b) Bolte, M.; Burguete, M. I.; Luis, S. V.; Alfonso, I.; Bru, M.; Rubio, J. *J. Am. Chem. Soc.* **2008**, *130*, 6137–6144; (c) Bolte, M.; Burguete, M. I.; Luis, S. V.; Alfonso, I.; Bru, M. *Chem.—Eur. J.* **2008**, *14*, 8879–8891; (d) Alfonso, I.; Burguete, M. I.; Luis, S. V.; Miravet, J. F.; Seliger, P.; Tomal, E. *Org. Biomol. Chem.* **2006**, *4*, 853–859; (e) Bru, M.; Burguete, M. I.; Luis, S. V.; Alfonso, I. *Angew. Chem., Int. Ed.* **2006**, *45*, 6155–6159; (f) Galindo, F.; Burguete, M. I.; Vigara, L.; Luis, S. V.; Kabir, N.; Gavrilovic, J.; Russell, D. A. *Angew. Chem., Int. Ed.* **2005**, *44*, 6504–6508.
8. (a) Luis, S. V.; Galindo, F.; Burguete, M. I.; Vigara, L. *J. Photochem. Photobiol., A* **2010**, *209*, 61–67; (b) Burguete, M. I.; Galindo, F.; Izquierdo, M. A.; Luis, S. V.; Vigara, L. *Dalton Trans.* **2007**, 4027–4033; (c) Galindo, F.; Becerril, J.; Burguete, M. I.; Luis, S. V.; Vigara, L. *Tetrahedron Lett.* **2004**, *45*, 1659–1662; (d) Bernardo, M. A.; Parola, A. J.; Pina, F.; García-España, E.; Luis, S. V.; Miravet, J. F. *J. Chem. Soc., Dalton Trans.* **1995**, 993–997.
9. (a) Feringa, B. L. *J. Org. Chem.* **2007**, *72*, 6635–6652; (b) Kay, E. R.; Leigh, D. A.; Zerbetto, F. *Angew. Chem., Int. Ed.* **2007**, *46*, 72–191; (c) Browne, W. R.; Feringa, B. L. *Nat. Nanotechnol.* **2006**, *1*, 25–35; (d) Kottas, G. S.; Clarke, L. I.; Horinek, D.; Michl, J. *Chem. Rev.* **2005**, *105*, 1281–1376; (e) Balzani, V.; Credi, A.; Venturi, M. *Molecular Devices and Machines-A Journey into the Nanoworld*; Wiley-VHC: Weinheim, Germany, 2003; (f) Stoddart, J. F. *Acc. Chem. Res.* **2001**, *34*, 410–411; (g) *Molecular Machines and Motors*; Sauvage, J. P., Ed.; Springer: Berlin, 2001; (h) Harada, A. *Acc. Chem. Res.* **2001**, *34*, 456–464.
10. (a) Alfonso, I.; Burguete, M. I.; Galindo, F.; Luis, S. V.; Vigara, L. *J. Org. Chem.* **2007**, *72*, 7947–7956; (b) Alfonso, I.; Burguete, M. I.; Luis, S. V. *J. Org. Chem.* **2006**, *71*, 2242–2250; (c) Albelda, M. T.; Bernardo, M. A.; Díaz, P.; García-España, E.; Seixas de Melo, J.; Pina, F.; Soriano, C.; Luis, S. V. *Chem. Commun.* **2001**, 1520–1521; (d) Bernardo, M. A.; Alves, S.; Pina, F.; de Melo, J. S.; Albelda, M. T.; García-España, E.; Llinares, J. M.; Soriano, C.; Luis, S. V. *Supramol. Chem.* **2001**, *13*, 435–445; (e) Alves, S.; Pina, F.; Albelda, M. T.; García-España, E.; Soriano, C.; Luis, S. V. *Eur. J. Inorg. Chem.* **2001**, 405–412.
11. (a) Luis, S. V.; Burguete, M. I.; Gaviña, F.; Costero, A. M.; Rebek, J. *Bioorg. Med. Chem. Lett.* **1991**, *1*, 87–88; (b) Gaviña, F.; Luis, S. V.; Costero, A. M.; Burguete, M. I.; Rebek, J. *J. Am. Chem. Soc.* **1988**, *110*, 7140–7143; (c) Rebek, J. *Acc. Chem. Res.* **1984**, *17*, 258–264; (d) Rebek, J.; Wattley, R. W.; Costello, T.; Gadwood, R.; Marshall, L. *J. Am. Chem. Soc.* **1980**, *102*, 7398–7400.
12. (a) Brandt, K.; Porwolik-Czomperlik, I.; Siwy, M.; Kupka, T.; Shaw, R. A.; Davies, D. B.; Hursthouse, M. B.; Sykara, G. D. *J. Am. Chem. Soc.* **1997**, *119*, 12432–12440; (b) Aarts, V. M. L. J.; Grootenhuis, P. D. J.; Reinhoudt, D. N.; Czech, A.; Czech, B. P.; Bartsch, R. *Recl. Trav. Chim. Pays-Bas* **1988**, *107*, 94–103; (c) Artz, S. P.; Cram, D. J. *J. Am. Chem. Soc.* **1984**, *106*, 2160–2171; (d) Reinhoudt, D. N.; de Joy, F.; van de Vondervoot, M. *Tetrahedron* **1981**, *37*, 1985–1990; (e) Reinhoudt, D. N.; de Joy, F.; van de Vondervoot, M. *Tetrahedron* **1981**, *37*, 1753–1762; (f) Helgerson, R. C.; Weisman, G. R.; Toner, J. L.; Tarnowski, T. L.; Chao, Y.; Mayer, J. M.; Cram, D. J. *J. Am. Chem. Soc.* **1979**, *101*, 4928–4941; (g) Kohama, H.; Yoshinaga, M.; Ishizu, K. *Bull. Chem. Soc. Jpn.* **1980**, *53*, 3707–3708.
13. (a) Burguete, M. I.; Escuder, B.; García-España, E.; López, L.; Luis, S. V.; Miravet, J. F.; Querol, M. *Tetrahedron Lett.* **2002**, *43*, 1817–1819; (b) Burguete, M. I.; Luis, S. V.; Miravet, J. F.; Querol, M.; García-España, E. *Chem. Commun.* **1999**, 649–650.
14. (a) Montero, A.; Albericio, F.; Royo, M.; Herradón, B. *Eur. J. Org. Chem.* **2007**, 1301–1308; (b) Choi, K.; Hamilton, A. D. *J. Am. Chem. Soc.* **2003**, *125*, 10241–10249; (c) Kuhnert, N.; Straûnig, C.; Lopez-Periago, A. M. *Tetrahedron: Asymmetry* **2002**, *13*, 123–128; (d) Costero, A. M.; Andreu, C.; Martínez-Máñez, R.; Soto, J.; Ochando, L. E.; Amigó, J. M. *Tetrahedron* **1997**, *54*, 8159–8170; (e) Patel, H. K.; Kilburn, J. D.; Langley, G. J.; Edwards, P. D.; Mitchell, T.; Southgate, R. *Tetrahedron Lett.* **1994**, *35*, 481–484.
15. Brandes, S.; Gros, C.; Denat, F.; Pullumbi, P.; Guilard, R. *Bull. Soc. Chim. Fr.* **1996**, *133*, 65–73.
16. García-España, E.; Ballester, M. J.; Lloret, F.; Moratal, J. M.; Faus, J.; Bianchi, A. *J. Chem. Soc., Dalton Trans.* **1988**, 101–104.
17. M. Fontanelli and M. Micheloni, Proceedings of the I Spanish-Italian Congress on Thermodynamics of Metal Complexes, Diputación de Castellón, Spain, 1990. Program for the automatic control of the microburette and the acquisition of the electromotive force readings; Diputación de Castellón.
18. Gans, P.; Sabatini, A.; Vacca, A. *Talanta* **1996**, *43*, 1739–1753.
19. For protonation and complex formation constants for cyclam, see: (a) Thom, V. J.; Hosken, G. D.; Hancock, R. D. *Inorg. Chem.* **1985**, *24*, 3378–3381; (b) Micheloni, M.; Sabatini, A. .; Paoletti, P. *J. Chem. Soc., Perkin Trans. 2* **1978**, 828–830.
20. (a) Chambron, J. C.; Meyer, M. *Chem. Soc. Rev.* **2009**, *38*, 1663–1673; (b) Szakacs, Z.; Kraszni, M.; Noszal, B. *Anal. Bioanal. Chem.* **2004**, *378*, 1428–1448; (c) Bencini, A.; Bianchi, A.; Garcia-España, E.; Micheloni, M.; Ramirez, J. A. *Coord. Chem. Rev.* **1999**, *188*, 97–156.
21. (a) Aran, V. J.; Kumar, M.; Molina, J.; Lamarque, L.; Navarro, P.; Garcia-España, E.; Ramirez, J. A.; Luis, S. V.; Escuder, B. *J. Org. Chem.* **1999**, *64*, 6135–6146; (b) Aguilar, J. A.; Garcia-España, E.; Guerrero, J. A.; Luis, S. V.; Llinares, J. M.; Ramirez, J. A.; Soriano, C. *Inorg. Chim. Acta* **1996**, *246*, 287–294; (c) Bianchi, A.; Escuder, B.; Garcia-España, E.; Luis, S. V.; Marcelino, V.; Miravet, J. F.; Ramirez, J. A. *J. Chem. Soc., Perkin Trans. 2* **1994**, 1253–1259.
22. (a) Dong, H.; Du, H.; Qian, X. *J. Phys. Chem. A* **2008**, *112*, 12687–12694; (b) Milletti, F.; Storchi, L.; Sforna, G.; Cruciani, G. *J. Chem. Inf. Model.* **2007**, *47*, 2172–2181; (c) Brown, T. N.; Mora-Diez, N. *J. Phys. Chem. B* **2006**, *110*, 20546–20554; (d) Brown, T. N.; Mora-Diez, N. *J. Phys. Chem. B* **2006**, *110*, 9270–9279; (e) Busch, M. S.; Knapp, E. W. *ChemPhysChem.* **2004**, *5*, 1513–1522.
23. Pople, J. A., et al. *Gaussian 03, Revision B.04*; Gaussian: Pittsburgh PA, 2003.
24. (a) Reed, A. E.; Weinstock, R. B.; Weinhold, F. *J. Chem. Phys.* **1985**, *83*, 735–746; (b) Reed, A. E.; Weinhold, F. *J. Chem. Phys.* **1983**, *78*, 4066–4073; (c) Foster, J. P.; Weinhold, F. *J. Am. Chem. Soc.* **1980**, *102*, 7211–7218.
25. For non-quaternized nitrogen atoms, their involvement in hydrogen bonding is defined when the calculated Wiberg Bond Index (WBI) is greater than 2.95.
26. (a) García-España, E.; Luis, S. V. *Supramol. Chem.* **1996**, *6*, 257–266; (b) Domenech, A.; Folgado, J. V.; Garcia-España, E.; Luis, S. V.; Llinares, J. M.; Miravet, J. F.; Ramirez, J. A. *J. Chem. Soc., Dalton Trans.* **1995**, 541–547; (c) Andrés, A.; Burguete, M. I.; García-España, E.; Luis, S. V.; Miravet, J. F.; Soriano, C. *J. Chem. Soc., Perkin Trans. 2* **1993**, 749–754.
27. Chand, D. K.; Schneider, H. J.; Aguilar, J. A.; Escartí, F.; García-España, E.; Luis, S. V. *Inorg. Chim. Acta* **2001**, *316*, 71–78.
28. Díaz, P.; García-España, E.; López, L.; Luis, S. V.; Querol, M. *Supramol. Chem.* **2002**, *2*, 107–114.
29. (a) Andres, S.; Escuder, B.; Domenech, A.; Garcia-España, E.; Luis, S. V.; Marcelino, V.; Llinares, J. M.; Ramirez, J. A.; Soriano, C. *J. Phys. Org. Chem.* **2001**, *14*, 495–500; (b) Altava, B.; Burguete, M. I.; Luis, S. V.; Miravet, J. F.; Garcia-España, E.; Marcelino, V.; Soriano, C. *Tetrahedron* **1997**, *53*, 4751–4762.
30. (a) Bazzicalupi, C.; Bencini, A.; Lippolis, V. *Chem. Soc. Rev.* **2010**, *39*, 3709–3728; (b) Mateus, P.; Delgado, R.; Brandão, P.; Félix, V. *J. Org. Chem.* **2009**, *74*, 8638–8646; (c) Anda, C.; Bazzicalupi, C.; Bencini, A.; Berni, E.; Bianchi, A.; Fornasari, P.; Llobet, A.; Giorgi, C.; Paoletti, P.; Valtancoli, B. *Inorg. Chim. Acta* **2003**, *356*, 167–178; (d) Beer, P. D.; Cadman, J.; Lloris, J. M.; Martínez-Máñez, R.; Padilla, M. E.; Pardo, T.; Smith, D. K.; Soto, J. *J. Chem. Soc., Dalton Trans.* **1999**, 127–133; (e) Lu, Q.; Reibenspies, J. H.; Carroll, R. I.; Martell, A. E.; Clearfiled, A. *Inorg. Chim. Acta* **1998**, *270*, 207–215; (f) Nation, D. A.; Reibenspies, J.; Martell, A. E. *Inorg. Chem.* **1996**, *35*, 4597–4603; (g) Motekaitis, R. J.; Martell, A. E. *Inorg. Chem.* **1992**, *31*, 5534–5542; (h) Dietrich, B.; Guilhem, J.; Lehn, J. M.; Pascard, C.; Sonveaux, E. *Helv. Chim. Acta* **1984**, *67*, 91–104.
31. Albelda, M. T.; Aguilar, J.; Aucejo, R.; Díaz, P.; Lodeiro, C.; Lima, J. C.; García-España, E.; Pina, F.; Soriano, C. *Helv. Chim. Acta* **2003**, *86*, 3118–3134; Albelda, M. T.; Bernardo, M. A.; García-España, E.; Godino, M.-L.; Luis, S. V.; Melo, M. J.; Pina, F.; Soriano, C. *J. Chem. Soc., Perkin Trans. 2* **1999**, 2545–2549.
32. Bazzicalupi, C.; Bencini, A.; Bianchi, A.; Cecchi, M.; Escuder, B.; Fusi, V.; García-España, E.; Giorgi, C.; Luis, S. V.; Maccagni, G.; Marcelino, V.; Paoletti, P.; Valtancoli, B. *J. Am. Chem. Soc.* **1999**, *121*, 6807–6815.
33. Albelda, M. T.; Frías, J. C.; García-España, E.; Luis, S. V. *J. Chem. Soc., Perkin Trans. 2* **2004**, 816–820.
34. Spartan'04; Wavefunction,: Irvine, CA, 2005.
35. (a) Rossotti, F. J.; Rossotti, H. *J. Chem. Educ.* **1965**, *42*, 375–378; (b) Gran, G. *Analyst (London)* **1952**, *77*, 671–681.